PNAS RESEARCH ARTICLE | NEUROSCIENCE

Somatostatin regulates central clock function and circadian responses to light

Deborah A. M. Joye[a], Kayla E. Rohr[a], Kimberlee Suenkens[a], Alissa Wuorinen[a], Thomas Inda[a], Madeline Arzbecker[a], Emma Mueller[a], Alec Huber[a], Harshida Pancholi[a], Murray G. Blackmore[a], Vania Carmona-Alcocer[a], and Jennifer A. Evans[a,1]

Edited by Erik D. Herzog, Washington University, St. Louis, MO; received October 2, 2022; accepted March 21, 2023 by Editorial Board Member Amita Sehgal

Daily and annual changes in light are processed by central clock circuits that control the timing of behavior and physiology. The suprachiasmatic nucleus (SCN) in the anterior hypothalamus processes daily photic inputs and encodes changes in day length (i.e., photoperiod), but the SCN circuits that regulate circadian and photoperiodic responses to light remain unclear. Somatostatin (SST) expression in the hypothalamus is modulated by photoperiod, but the role of SST in SCN responses to light has not been examined. Our results indicate that SST signaling regulates daily rhythms in behavior and SCN function in a manner influenced by sex. First, we use cell-fate mapping to provide evidence that SST in the SCN is regulated by light via de novo *Sst* activation. Next, we demonstrate that *Sst*$^{-/-}$ mice display enhanced circadian responses to light, with increased behavioral plasticity to photoperiod, jetlag, and constant light conditions. Notably, lack of *Sst*$^{-/-}$ eliminated sex differences in photic responses due to increased plasticity in males, suggesting that SST interacts with clock circuits that process light differently in each sex. *Sst*$^{-/-}$ mice also displayed an increase in the number of retinorecipient neurons in the SCN core, which express a type of SST receptor capable of resetting the molecular clock. Last, we show that lack of SST signaling modulates central clock function by influencing SCN photoperiodic encoding, network after-effects, and intercellular synchrony in a sex-specific manner. Collectively, these results provide insight into peptide signaling mechanisms that regulate central clock function and its response to light.

circadian | photoperiod | suprachiasmatic nucleus | somatostatin | behavior

Significance

Light impacts human health by reprogramming the central circadian clock. Circadian responses to light coordinate behavior and physiology so that it is adjusted to daily and seasonal changes in the environment. Our work indicates that circadian responses to light are modulated by somatostatin, a peptide widely expressed in the brain. We show that light modulates the neurochemistry of central clock circuits, with long days increasing somatostatin expression. Further, we show that lack of somatostatin increases circadian plasticity at the behavioral and cellular levels. Last, our work reveals sex differences in circadian responses to light and the role of somatostatin. Further work comparing photic processing in both sexes can provide better insight into gender differences in circadian responses to light.

Light modulates brain function in ways that can benefit or disrupt human health. Daytime light exposure is critical for the optimal regulation of daily rhythms, but light at night increases the risk for pathology (1). Aberrant light exposure affects an estimated 15 to 80% of people due to shiftwork, light pollution, and nighttime device use (2–4). In addition, human health is influenced by the *duration* of daily light exposure (i.e., photoperiod). Neuropsychiatric disorders display annual fluctuations in symptoms that vary systematically across latitude and hemisphere (5). This suggests that daily and annual changes in light exposure modulate neural function in humans, but the mechanisms by which light can cause adaptive and maladaptive plasticity in neural circuits remain poorly defined.

Circadian and photoperiodic responses to light require the suprachiasmatic nucleus (SCN), which is the central daily clock and annual calendar in mammals (6, 7). At the cellular level, circadian timekeeping is driven by transcriptional–translational feedback loops that program daily rhythms in gene expression and cellular physiology. Daily light cues reset the SCN molecular clock, with initial processing in SCN core neurons that express GABA and the neuropeptides vasoactive intestinal polypeptide (VIP) and gastrin-releasing peptide (GRP, refs. 8–10). Photic inputs are processed and transmitted to the broader SCN circuit, then ultimately the larger circadian system to influence the phase, period, and waveform of daily rhythms (7). Photoperiodic plasticity in the waveform and period of daily rhythms in behavior is associated with reprogramming of SCN circuits and intercellular signaling (6, 7). SCN photoperiodic encoding is influenced by both VIP and GABA signaling (11–13), but the network-level circuits that regulate circadian responses to light have not been fully mapped.

Somatostatin (SST) is an inhibitory neuropeptide produced by a subpopulation of SCN neurons with extensive intra-network connections (9, 14, 15). Widely expressed in the brain, SST acts via a family of five SST receptors (SSTR) coupled to $G_{i/o}$ signaling. Changes in SST signaling are linked to neuropsychiatric disorders with circadian and seasonal components in humans and rodent models (5, 16). Further, photoperiod modulates SST expression in the rodent hypothalamus, with SST levels in the paraventricular nucleus (PVN) and periventricular nucleus (PeVN) associated with light-driven changes

Author contributions: D.A.M.J., K.E.R., K.S., T.I., M.A., V.C.-A., and J.A.E. designed research; D.A.M.J., K.E.R., K.S., A.W., T.I., M.A., E.M., A.H., H.P., V.C.-A., and J.A.E. performed research; M.G.B. and J.A.E. contributed new reagents/analytic tools; D.A.M.J., K.E.R., K.S., A.W., T.I., M.A., E.M., A.H., H.P., V.C.-A., and J.A.E. analyzed data; J.A.E. directed research; and D.A.M.J. and J.A.E. wrote the paper.

The authors declare no competing interest.

This article is a PNAS Direct Submission. E.D.H. is a guest editor invited by the Editorial Board.

[1]To whom correspondence may be addressed. Email: jennifer.evans@marquette.edu.

This article contains supporting information online at https://www.pnas.org/lookup/suppl/doi:10.1073/pnas.2216820120/-/DCSupplemental.

Published April 25, 2023.

in depression- and anxiety-like behavior (17–19). This work suggests that light is able to reprogram neural identity by causing neurons to switch neurotransmitter expression between SST and dopamine. Recent work indicates that the SCN drives this downstream SST–dopamine neurotransmitter switching in the PVN (20), but it has not been tested whether SST influences the function of the circadian clock, its response to light, or changes with photoperiod.

Here, we test that SST influences circadian and photoperiodic responses to light. First, we map *Sst* neurons in the SCN network, providing genetic evidence that long days increase SCN SST expression via de novo *Sst* transcription. Next, we show that germline SST knockout mice ($Sst^{-/-}$) display enhanced circadian responses to light at the behavioral and cellular levels. Interestingly, sex differences in behavioral and cellular responses to light were eliminated in $Sst^{-/-}$ mice due to enhanced plasticity in males. Collectively, these data indicate that SCN SST levels are regulated by light, and that SST signaling acts to increase circadian robustness in a sexually dimorphic manner.

Results

Spatiotemporal Mapping of Sst Expression in the SCN. First, we examined spatial patterning of SCN *Sst*-expressing neurons using a genetic approach (Fig. 1*A* and *SI Appendix*, Fig. S1 *A* and *B*). The majority of *Sst*–tdT+ neurons were in the dorsal regions of the posterior SCN shell (Fig. 1*A* and *SI Appendix*, Fig. S1*A*), consistent with (9). Overall, SCN *Sst*–tdT+ cells were fewer in number than those labeled by *Vip*–tdT+ and *Avp*–tdT+ (*SI Appendix*, Fig. S1 *C–E*). In the sagittal plane, *Sst*–tdT+ cells were also located dorsal and posterior to the SCN (*SI Appendix*, Fig. S1*A*), but *Sst*–tdT+ neurons in the SCN were smaller than those in surrounding structures (*SI Appendix*, Fig. S1*B*, $F(2, 9) = 7.65$, $P = 0.01$, Tukey's HSD, $P < 0.05$). *Sst*–tdT labeling was complemented with SST immunohistochemistry (IHC) at four time points spanning the LD12:12 (L12) photocycle (Fig. 1 *A–D* and *SI Appendix*, Fig. S2 *A* and *B*). Independent of time, approximately 77% of *Sst*–tdT+ cells expressed SST above background (Fig. 1*B*). SST was also expressed in fiber-like processes clustered in the SCN core, but not *Sst–tdT*+ tracts in the optic nerve (Fig. 1*A* and *SI Appendix*, Fig. S1*C*).

Further, daily expression of SST and *Sst* was rhythmic in the SCN (Fig. 1*C* and *SI Appendix*, Fig. S2), consistent with previous work (21, 22). SST protein expression was rhythmic at the whole SCN level (Fig. 1*C*; $F(2, 28) = 6.3$, $P = 0.004$), with higher amplitude rhythms in posterior slices (*SI Appendix*, Fig. S2*B*). Cellular SCN expression of SST was also rhythmic (*SI Appendix*, Fig. S2*C*, $t(28) = 3.13$, $P = 0.004$), with a daytime peak in the percentage of *Sst*–tdT+ cells coexpressing SST (Fig. 1*D*; $t(29) = 2.7$, $P = 0.01$). The number of SCN *Sst*–tdT+ cells did not fluctuate (*SI Appendix*, Fig. S2*C*, $t(28) = 0.9$, $P = 0.4$), consistent with permanent tdT labeling after the onset of transcription (23). At the transcript level, *Sst* was also expressed largely in the posterior SCN shell, with elevated expression during the night (Fig. 1*C* and *SI Appendix*, Fig. S2 *D* and *E*, $F(3, 213) = 5.11$, $P = 0.007$). SCN SST and *Sst* expression differed by sex, with daily rhythms detected in males but not females (*SI Appendix*, Fig. S2 *E* and *F*). Overall, these results indicate that SST and *Sst* are rhythmically expressed in a subset of SCN neurons in a manner that differs by sex.

SCN SST Expression Is Modulated by Photoperiod. Next, we examined whether SCN SST levels vary with photoperiod, as seen in other hypothalamic structures (17–19). Mice were entrained

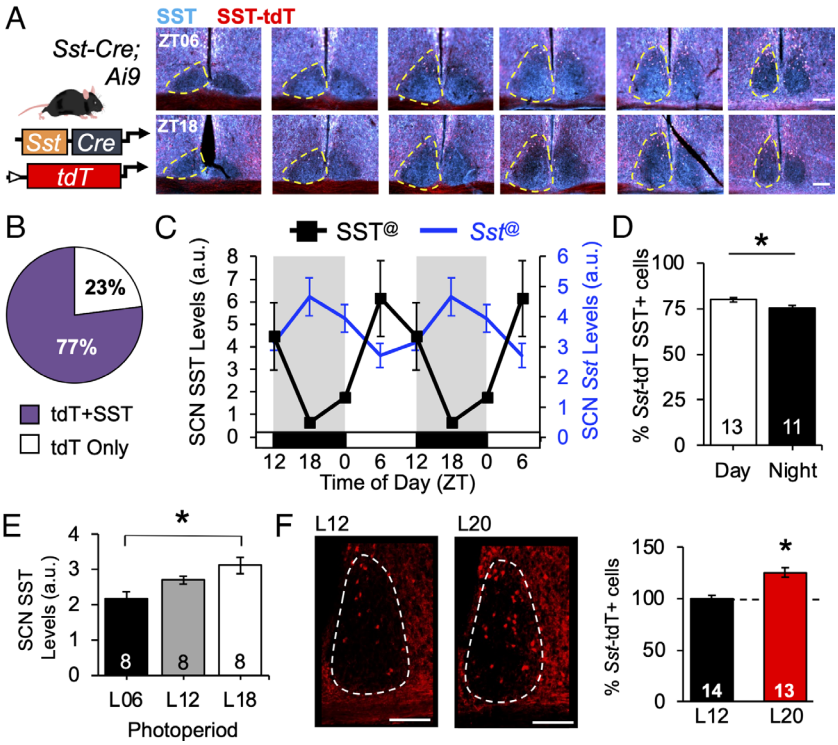

Fig. 1. Spatiotemporal mapping of *Sst* SCN subpopulation. (*A*) Genetic approach for labeling *Sst*–tdT+ cells, with representative images illustrating *Sst*–tdT and SST expression at midday (ZT06) and midnight (ZT18). (*B*) Percent cells expressing *Sst*–tdT with and without SST. (*C*) Daily rhythm in SST and *Sst* expression, double-plotted to facilitate visualization. (*D*) Day–night difference in SCN expression of *Sst*–tdT and SST. (*E*) Photoperiodic modulation of SCN SST expression. (*F*) Photoperiodic modulation of *Sst* transcription in the hypothalamus. Representative images illustrating SCN *Sst*–tdT+ cells. Twelve weeks of L20 entrainment increased the number of SCN *Sst*–tdT+ cells. Scale bars, 100 μm, ZT = Zeitgeber time, ZT12 = time of lights off, a.u. = arbitrary units. @Circwave test of rhythmicity, $P < 0.05$. *post hoc comparisons, $P < 0.05$.

to short (6 h of light/day, L06), control (L12), or long-day photoperiods (L18) prior to receiving 1 µl colchicine injections into the third ventricle to slow microtubule transport and visualize total peptide production over the circadian cycle. SST levels in SCN cells were proportional to day length (Fig. 1*E* and *SI Appendix*, Fig. S3*A*, PP: F (2, 17) = 7.8, P = *0.004*, Sex: F (1, 17) < 0.1, P = 0.95, PP*Sex: F (2, 17) = 2.3, P = 0.14). In the PeVN, SST expression also varied with photoperiod, but in a manner that interacted with sex (*SI Appendix*, Fig. S3*A*, PP*Sex: F (2, 17) = 7.0, P = *0.006*). Next, we tested whether photoperiod modulates daily rhythms in SCN SST expression by exposing male mice to extreme long-day photocycles with 20 h of light (L20). SST rhythms in the male SCN were affected by L20 (*SI Appendix*, Fig. S3 *B* and *C*, PP*ZT: F (3, 90) = 4.4, P = *0.006*), with increased expression at the times corresponding to dawn and dusk in L12 (*SI Appendix*, Fig. S3*C*, LSM Contrasts, P < *0.05*). Collectively, these results indicate that SCN SST levels and rhythms are modulated by photoperiod.

To assess whether long days increase SST via de novo *Sst* transcription, *Sst*–tdT mice were exposed to L12 or L20 for 12 wk. We predicted that the number of *Sst*–tdT+ labeled cells would be higher in L20 than that in L12 if long days activate nascent *Sst* transcription. Sex influenced the number of *Sst*–tdT+ cells under L12 (*SI Appendix*, Fig. S3*D*), so data were normalized to sex-matched controls to evaluate L20 patterns in both sexes (Fig. 1*F*). L20 exposure for 12 wk increased the number of *Sst*–tdT+ cells in the SCN by 25% (Fig. 1*F*, PP: t (23) = 4.7, P = *0.0001*), with the largest increase in the middle and posterior SCN (*SI Appendix*, Fig. S3*H*). In agreement with previous work, L20 also increased *Sst*–tdT+ cells in the PVN by 34% (*SI Appendix*, Fig. S3 *E–H*, t (20) = 2.7, P = *0.0001*), but we did not detect consistent changes in the PeVN (*SI Appendix*, Fig. S3 *E–H* t (13) = 0.7, P > 0.4). When divided by sex, exposure to L20 first elevated *Sst*–tdT cell counts in the SCN and PVN by 6 and 8 wk, respectively (*SI Appendix*, Fig. S3*I*), and there were sex differences in the timing and patterning of this response. Collectively, these results indicate that *Sst* is modulated by photoperiod via de novo transcription in both the SCN and PVN.

SST Regulates Photoperiodic Changes in Circadian Behavior. Next, we tested that SST is necessary for photoperiodic modulation of daily rhythms in locomotor behavior (Fig. 2*A* and *SI Appendix*, Fig. S4*A*). Photoperiod modulates the phasing, waveform, and period of circadian rhythms (24). Under different photoperiods, circadian waveform is typically measured by the duration of wake versus sleep over the daily photocycle. In rodents, the duration of locomotor activity (i.e., alpha) is proportional to the duration of darkness (i.e., scotophase). Systemic changes in alpha are indicative of photoperiodic entrainment, but light can also acutely suppress or "mask" locomotor activity. Release into DD establishes effects of photoperiod in central clock circuits, with after-effects in both circadian waveform and period. *Sst*$^{-/-}$ founder mice were provided generously by Dr. Malcolm Low (25, *SI Appendix*, Fig. S2*A*). Body weight (Females: F (2, 26) = 0.04, P = 0.97; Males: F (2, 26) = 0.14, P = 0.8), levels of wheel-running activity (*SI Appendix*, Fig. S4*B*), and L12 entrainment did not differ by genotype (Fig. 2 *A* and *B* and *SI Appendix*, Fig. S4 *C–E*). This indicates that basic physiology and photoentrainment were intact in *Sst*$^{-/-}$ mice, consistent with previous work (25, 26).

Relative to controls, *Sst*$^{-/-}$ mice displayed larger photoperiodic responses under both long and short days (Fig. 2 *A* and *B* and *SI Appendix*, Fig. S4*D*). Under long days, *Sst*$^{-/-}$ mice displayed greater alpha compression over time (Fig. 2 *A* and *B* and *SI Appendix*, Fig. S4 *D* and *E*, GT*Week: F (18, 450) = 2.3, P = *0.002*; LSM Contrasts, P < *0.002*), and photophase activity levels were lower in

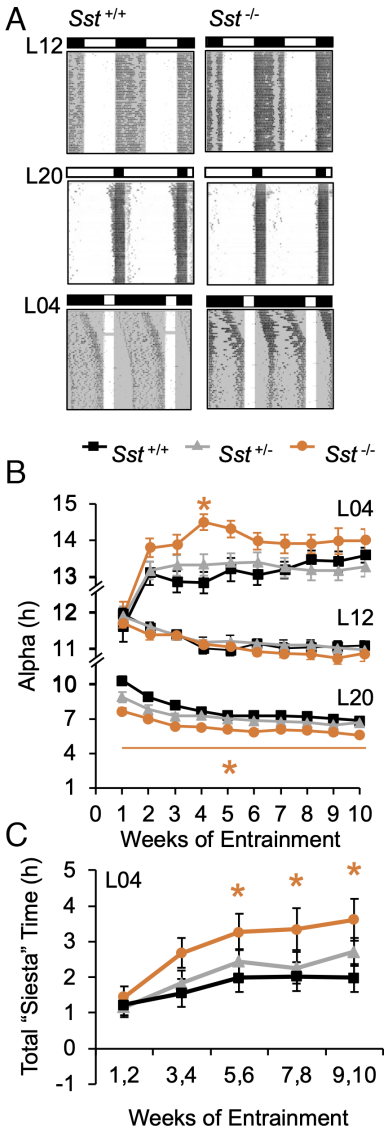

Fig. 2. Lack of SST enhances photoperiodic modulation of circadian waveform. (*A*) Representative double-plotted wheel-running actograms from male mice of each group. Lighting conditions are illustrated with white:black bars and internal shading. (*B*) Photoperiodic modulation of circadian waveform during entrainment. (*C*) Photoperiodic modulation of daily siesta time during entrainment. *post hoc comparisons, P < *0.05*.

Sst$^{-/-}$ mice (*SI Appendix*, Fig. S4*G*). Notably, genotype influenced peri-dawn and -dusk activity levels that tracked reentrainment of activity into the scotophase (*SI Appendix*, Fig. S4*H*). Under short days, mice displayed individual differences in the phase angle of entrainment independent of genotype (*SI Appendix*, Fig. S4*A*). As expected, alpha expanded in all groups, and the rate of alpha expansion was initially greater in *Sst*$^{-/-}$ mice (Fig. 2*B* and *SI Appendix*, Fig. S4*D*, GT: F (2, 55) = 3.5, P = *0.04*, Week: F (9, 495) = 24.6, P < 0.0001; GT*Week: F (18, 495) = 1.5, P = 0.08; LSM Contrasts, Wk4: P < *0.0005*, Wk3: P = *0.05*, Wk5: P = *0.03*). Under both long and short days, genotypic differences in circadian waveform were driven by changes in activity offset (*SI Appendix*, Fig. S4 *C* and *D*). Further, genotype influenced sex- and photoperiod-specific changes in the architecture of locomotor rhythms (Fig. 2*C* and *SI Appendix*, Fig. S4*F*). Consistent with previous work (27), male mice displayed more consistent nightly "siestas" (i.e., inactive interval during the scotophase; *SI Appendix*, Fig. S4*A*; Sex: F (1, 146) = 43.3, P < *0.0001*). Exposure to short days increased "siesta" duration in males (PP: F (2, 146) = 32.3, P < *0.0001;* PP*Wk: F (8, 584) =

2.3, $P < 0.05$; PP*Sex: F (2, 146) = 13.0, $P < 0.0001$), with male $Sst^{-/-}$ mice displaying the largest increases (Fig. 2*C* and *SI Appendix*, Fig. S4*F*, LSM Contrasts, $P < 0.05$). Given that activity levels did not differ by genotype (*SI Appendix*, Fig. S4*B*), this pattern of results suggests that lack of SST affects the daily distribution of activity rather than masking.

To test photoperiodic after-effects indicative of central clock function, mice were released from each photoperiod into constant darkness (DD, *SI Appendix*, Fig. S5*A*). As expected, mice released from long days quickly expanded alpha over the first week of DD. Over the next 2 wk, $Sst^{-/-}$ mice displayed a greater rate of alpha expansion relative to controls (*SI Appendix*, Fig. S5*B*, GT: F (2, 40) = 5.2, $P < 0.01$, LSM Contrasts, $P < 0.01$), which ultimately normalized alpha across groups (*SI Appendix*, Fig. S5*B*). In contrast, genotype did not influence photoperiodic after-effects in circadian period (*SI Appendix*, Fig. S5*C*, PP: F (2, 151) = 285.42, $p < 0.0001$; GT: F (2, 151) = 2.1, P = 0.12, PP*GT: F (4, 151) = 3.2, $P = 0.01$; post hoc ANOVA: GT: L12- $P > 0.1$, L20- $P > 0.1$, L04- $P > 0.1$). Following an extended free-run, phase resetting responses to short, 20 min light pulses differed by circadian phase and sex (*SI Appendix*, Fig. S5*D*, Sex: F (1, 292) = 4.8, $P = 0.03$; CT: F (3, 292) = 157.3, $P = 0.0001$; Sex*CT: F (3, 292) = 6.4, $P = 0.0005$), but photic resetting was not affected by photoperiod or genotype (PP: F (2, 292) = 1.4, $P > 0.2$; GT: F (2, 292) = 1.9, $P > 0.1$, PP*GT: F (4, 292) = 1.5, $P > 0.2$). Collectively, these results suggest that SST modulates circadian responses to light that differ from those required for discrete photic resetting and period after-effects.

To examine other types of circadian responses to light, we tested genotype differences during simulated jetlag and constant light (LL, Fig. 3 and *SI Appendix*, Fig. S6). In both behavioral assays, females displayed larger responses than males, and lack of SST eliminated this sex difference by potentiating responses in males. During simulated eastward travel, locomotor activity rhythms reentrained through phase advances of activity onset in all groups (Fig. 3*A* and *SI Appendix*, Fig. S6), with days to recovery defined as the day on which activity onset advanced by 6 h. Both sex and genotype influenced the rate of reentrainment (Fig. 3*B*, GT: F (2, 54) = 6.9, $P < 0.005$, Sex: F (1, 54) = 12.3, $P < 0.001$; GT*Sex: F (1, 54) = 2.4, P = 0.09). Consistent with previous work (28), females reentrained in a fewer number of days relative to wild-type males (Fig. 3*B*, LSM Contrasts, $P < 0.05$). When effects of genotype were assessed separately by sex, male $Sst^{-/-}$ mice displayed accelerated recovery from jetlag (Fig. 3*B*, F (2, 27) = 7.9, $P < 0.005$), but lack of *Sst* did not further accelerate responses in females (Fig. 3*B*, F (2, 27) = 1.5, $P > 0.1$). Similarly, under LL, wild-type females displayed higher rates of arrhythmia compared to wild-type males (Fig. 3*C*, $\chi^2(1) = 3.8$, $P = 0.006$). Lack of *Sst* increased the incidence of LL-induced arrhythmia in males, but not females (Fig. 3*C*, Male: $\chi^2(1) = 7.6$, $P = 0.006$, Female: $\chi^2(1) = 0.6$, P = 0.4). However, the power of the free-running rhythm was lower in $Sst^{-/-}$ mice of each sex (Fig. 3*D*, LSM Contrasts, $P < 0.01$). Overall, lack of $Sst^{-/-}$ eliminated the sex difference in jetlag and LL behavior observed in wild-type mice (Fig. 3 *B* and *C*, LSM Contrasts, $P > 0.1$, $\chi^2(1) = 0.8$, $P > 0.3$). Collectively, these results suggest that SST modulates photic responses under circadian assays indicative of SCN reprogramming (7).

Lack of SST Alters SCN Function and Neurochemistry. To determine whether SST influences SCN function, we first examined genotypic differences in SCN neurochemistry after colchicine

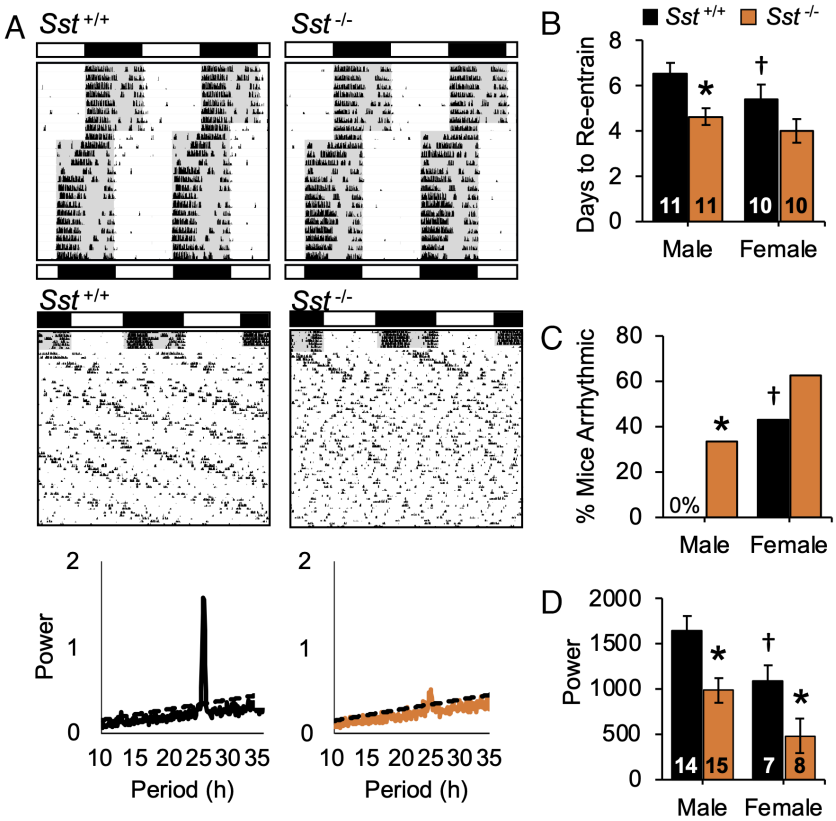

Fig. 3. Lack of SST enhances circadian responses to light. (*A*) Representative double-plotted wheel-running actograms from male mice exposed to simulated jetlag (6 h advance) and constant light (LL). Lighting conditions are illustrated with white:black bars and internal shading. *post hoc comparisons, $P < 0.05$. (*B*) Days to reentrain to new LD cycle. (*C-D*) Incidence of LL-induced arrhythmia and power of χ^2 periodogram. †Wild-type sex difference, *Genotype difference, post hoc comparisons, $P < 0.05$.

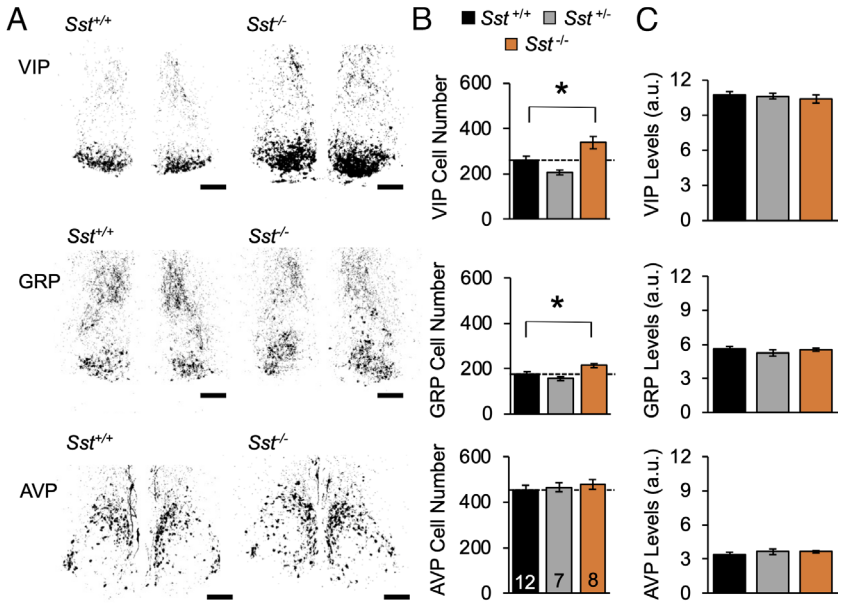

Fig. 4. Lack of SST increases the number of SCN VIP and GRP neurons. (*A*) Representative, thresholded images illustrating total peptide expression. (*B*) Average number of cells/sample. (*C*) Average cellular peptide levels. Male n = 4 to 9 mice/genotype, Female n = 3 mice/genotype. Scale bars, 100 μm, a.u. = arbitrary units. *post hoc comparisons, $P < 0.05$.

injections into the third ventricle (Fig. 4*A* and *SI Appendix*, Fig. S7). Under L12, lack of SST increased the number of SCN core neurons expressing VIP and GRP by 30% and 20%, respectively (Fig. 4*B*, VIP: $F(2, 24) = 9.7$, $P = 0.0008$; GRP: $F(2, 24) = 7.1$, $P = 0.004$). No change was detected in the number of AVP cells (Fig. 4*B*, $F(2, 24) = 0.4$, $P > 0.6$). Peptide levels were not affected by genotype (Fig. 4*C*, VIP: $F(2, 24) = 0.2$, $P > 0.8$; GRP: $F(2, 24) = 0.1$, $P > 0.9$; AVP: $F(2, 24) = 0.2$, $P > 0.7$), suggesting that SST regulates the number of retinorecipient neurons in the SCN core. Next, to test that SCN neurons can respond to SST signaling, we measured SCN expression of *Sstr1–4* (Fig. 5*A*). Highest in situ signals were detected for *Sstr1* (Fig. 5*A*, $t(4) = 4.6$, $P < 0.01$). In addition, *Sstr3* and *Sstr4* were also expressed above background levels (Fig. 5*A*, *Sstr3*: $t(5) = 3.4$, $P < 0.02$; *Sstr4*: $t(5) = 2.57$, $P < 0.05$). Each SST receptor displayed modest day–night differences, with *Sstr1* above background at both dusk and dawn (*SI Appendix*, Fig. S8*A*). These results demonstrate that SCN neurochemistry is modulated by the lack of *Sst* and the SCN expresses transcripts for SSTR.

Given that lack of *Sst* modulated SCN VIP/GRP cell number, we next investigated whether these retinorecipient SCN neurons express *Sstr1* (Fig. 5 *B* and *C* and *SI Appendix*, Fig. S8 *B–E*). As expected, *Vip* and *Grp* neurons were located primarily in the middle SCN (*SI Appendix*, Fig. S8*B*, (9), with daily rhythms in peptide transcription that differed by sex (*SI Appendix*, Fig. S8*D*), consistent with previous work (28). Important for colocalization, the number of *Vip*- and *Grp*- neurons detected did not vary across time of day (*SI Appendix*, Fig. S8*C*). Both *Vip*- and *Grp*- SCN neurons expressed *Sstr1*, with a larger percentage of *Vip* neurons expressing *Sstr1* relative to *Grp* neurons (Fig. 5*C*, $t(231) = 2.3$, $P < 0.0001$). Compared to females, males displayed a higher percentage of SCN *Vip* cells expressing *Sstr1* (Fig. 5*C*, $t(114) = 2.6$, $P = 0.01$), but the percentage of *Sstr1*-expressing *Grp* neurons did not differ by sex (Fig. 5*C*, $t(114) = 1.0$, $P > 0.3$). Further, *Sstr1* expression was rhythmic in both SCN *Vip* and *Grp* neurons in males (*SI Appendix*, Fig. S8*E*, *VipSstr1-* $F(3, 50) = 4.6$, $P < 0.05$, *GrpSstr1-* $F(3, 50) = 12.5$, $P < 0.0001$), but *Sstr1* expression in females was only rhythmic in SCN *Vip* neurons (*SI Appendix*, Fig. S8*E*, *VipSstr1-* $F(3, 60) = 3.5$, $P < 0.05$; *GrpSstr1-* $F(3, 60) = 1.6$, $P = 0.2$). Interestingly, sex differences in the timing of maximum *Sstr1* expression matched those in maximal *Vip* and *Grp* expression (*SI Appendix*, Fig. S8*D*). Overall, these results indicate that *Sstr1* is expressed in SCN core neurons, which may modulate SCN clock function and circadian responses to light differently in each sex.

Next, we tested whether SSTR1 signaling influences SCN molecular clock function by administering the selective SSTR1 agonist CH-275 (1 μm) ex vivo to SCN slices collected from L12 PER2::LUC mice (*SI Appendix*, Fig. S9*A*). Three consecutive slices were collected from the anterior, middle, and posterior SCN to test regional differences in molecular response. Administration of CH-275 at ZT12 phase delayed PER2::LUC rhythms specifically in middle SCN slices of each sex (*SI Appendix*, Fig. S9*B*, mSCN- $F(1, 16) = 9.8$, $P = 0.01$; aSCN- $F(3, 15) = 0.2$, $P > 0.9$; pSCN- $F(3, 14) = 1.7$, $P > 0.2$). In addition, CH-275 increased the amplitude of PER2::LUC rhythms in the posterior SCN on the cycle following administration (*SI Appendix*, Fig. S9*C*). In contrast, CH-275 treatment did not modulate SCN period (*SI Appendix*, Fig. S9*D*), matching results at the behavioral level (*SI Appendix*, Fig. S5*C*). These data indicate that SSTR1 signaling can influence SCN gene expression and reset the molecular clock.

Lack of SST Modulates SCN Network Responses to Long-Day Photoperiods. To test how SST influences SCN responses to photoperiod, $Sst^{-/-}$ mice were crossed to PER2::LUC mice and entrained to either L12 or L20 for ex vivo SCN bioluminescence imaging (Fig. 6*A* and *SI Appendix*, Fig. S10*A*). We collected tissue after 4 wk of entrainment because this was the timepoint when behavior first stabilized in each genotype under long days (Fig. 2*B*). Lack of *Sst* influenced both behavioral and SCN responses to L20 (Fig. 6 *B* and *C*), but no genotype differences were detected after L12 (*SI Appendix*, Fig. S10*B*). Behaviorally, alpha was again shorter in L20 $Sst^{-/-}$ mice (Fig. 6*B*, GT: $F(2, 46) = 10.6$, $P < 0.005$), although here this effect was driven by males (Fig. 6*B*, Sex: $F(1, 46) = 11.5$, $P < 0.005$, GT*Sex: $F(1, 46) = 5.3$, $P < 0.05$, LSM Contrasts, Male: $P = 0.0002$; Female: $P = 0.5$). Consistent with these behavioral results, the effect of $Sst^{-/-}$ on SCN responses to L20 differed by sex (Fig. 6*C*; GT:

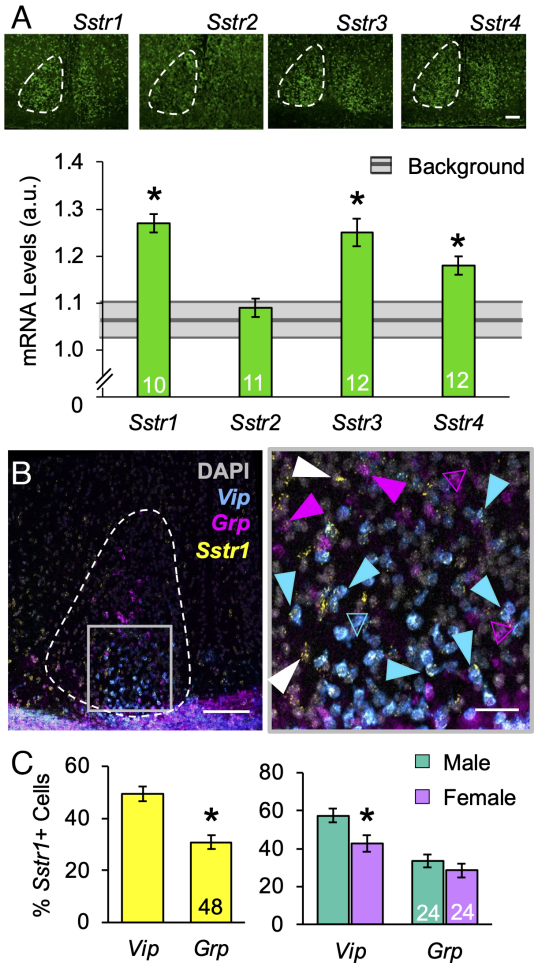

Fig. 5. SCN expression of SSTR. (*A*) Representative images of *Sstr1-4* expression and levels in the SCN. Gray bar indicates background levels for each probe ± the 95% (CI). (*B*) Representative image illustrating SCN transcription of *Vip, Grp,* and *Sstr1* at ZT18. At higher magnification, *Vip/Grp* cells with and without *Sstr1* coexpression are indicated by closed and open arrows, respectively. (*C*) Number of *Sstr1*-expressing *Vip* and *Grp* SCN neurons. Scale bar, 100 μm, Higher-magnification Scale bar, 25 μm *post hoc comparisons, $P < 0.05$.

F (1, 78) = 4.0, $P < 0.05$, Sex*GT: F (2, 78) = 5.0, $P < 0.05$). Specifically, male L20 $Sst^{-/-}$ mice displayed a larger phase difference between the SCN core and shell relative to controls (Fig. 6*C*, LSM Contrasts, $P = 0.0002$). Wild-type females displayed larger SCN responses compared to male counterparts (Fig. 6*C*, LSM Contrasts, $P = 0.005$), and lack of *Sst* did not further augment this response (Fig. 6*C*, LSM Contrasts, $P = 0.4$). SCN period after ex vivo release from L20 did not differ by genotype (Fig. 6*D*, F (3, 44) = 0.7, $P < 0.5$), also consistent with behavior (*SI Appendix*, Fig. S5*C*). Taken together, these results indicate that SST regulates SCN photoperiodic encoding and that this central clock network is sexually dimorphic in its photoperiodic response.

SST could modulate SCN response to long days by altering photic processing and/or local network function. To evaluate how SST signaling modulates SCN circuitry, PER2::LUC mice of each genotype were exposed to L20 for at least 8 wk to maximize SCN organization to analyze photoperiodic after-effects driven by network coupling ex vivo (13). In all groups, the SCN core and shell displayed a large phase difference on the first cycle in vitro, with changes in this phase relationship over time in culture (Fig. 7*A*). As expected (13), the coupling response curve describing these changes in SCN organization was biphasic in males (Fig. 7 *B* and *C*), with a negative zone in which SCN core neurons delay to resynchronize with the SCN shell and a positive zone in which SCN core neurons advance to resynchronize. In wild-type mice, sex influenced the shape of this coupling response curve, with a smaller positive zone in females (Fig. 7 *D* and *E*). When divided by sex, lack of *Sst* influenced SCN synchronization specifically in males (Fig. 7 *B*–*E*), with a reduction in the positive zone for male $Sst^{-/-}$ SCN (+AUC: t (16) = −5.8, $P < 0.001$; -AUC: t (16) = 0.4, $P > 0.1$) and no change for the female $Sst^{-/-}$ SCN (+AUC: t (12) = 0.3, $P > 0.1$; -AUC: t (12) = −1.65, $P > 0.1$). These results indicate that lack of SST modulates male SCN responses to long days; however, changes in network after-effects in this sex could reflect genotypic differences in the history of photoperiodic entrainment.

Last, to test the influence of SST signaling on SCN coupling while controlling for developmental and photoperiodic history, male PER2::LUC mice were exposed to L20 or L12 for at least 8 wk (*SI Appendix*, Fig. S10*C*). SCN slices were collected and cultured with or without a broad-spectrum SSTR antagonist (cyclosomatostatin, CSST, 20 μM). CSST administration to wild-type L12 SCN slices did not alter the phase or period of PER2::LUC rhythms (t (8) = 0.8, $P > 0.4$; t (8) = 0.6, $P > 0.6$). In contrast, CSST modulated SCN function after L20 exposure (*SI Appendix*, Fig. S10 *C* and *D*). On the first full cycle after tissue collection, CSST increased the phase difference between SCN neurons in the core and shell region (*SI Appendix*, Fig. S10*C*, t (17) = 4.3, $P < 0.001$), similar to the effects of germline *Sst* deletion in males (Fig. 6). Further, CSST blunted network resynchronization when the phase difference between SCN core and shell was maximal (*SI Appendix*, Fig. S10 *C* and *D*), also consistent with genetic results (Fig. 7*C*). Specifically, CSST reduced the positive zone of the coupling response curve for the male SCN (*SI Appendix*, Fig. S10*D*, +AUC: t (12) = 13.5, $P < 0.001$; -AUC: t (12) = 6.3, $P < 0.001$), suggesting that SST signaling modulates intercellular communication and network synchrony in the male SCN.

Discussion

Light modulates neural circuits that program daily and annual rhythms in behavior and physiology. Here, we complement and extend previous work showing that light modulates SCN neurochemistry by providing genetic evidence for photic activation of de novo *Sst* transcription in the central circadian clock. Further, this work reveals that SST signaling modulates circadian responses to light at the behavioral and cellular levels in a sexually dimorphic manner. At the behavioral level, we find that germline deletion of *Sst* enhanced circadian responses to light and eliminated sex differences due to increased plasticity in males. Consistent with this phenotype, loss of SST signaling augmented SCN responses to light and inhibited SCN coupling specifically in males. Collectively, these results highlight a mechanism whereby light activates a repressive peptide that modulates circadian responses to light and interacts with central clock circuits that differ by sex.

Here, we show that photoperiod modulates SST levels, daily SST rhythms, and the number of *Sst* cells in the SCN. Light, food, and hormonal signaling can modulate hypothalamic neurochemistry (17, 18, 29), with the suggestion that neurotransmitter switching may be bioenergetically favorable to structural rewiring in homeostatic circuits. Neuronal activity has been shown to be required for neurotransmitter switching (30), but the precise mechanisms driving de novo *Sst* transcription in the hypothalamus require further study. Our data indicate that long days increase SCN SST expression during dawn/dusk transitions, which may be driven by light-induced increases in SCN electrical activity and gene expression at these times of day (7). Further, previous work indicates that light can induce epigenetic changes in SCN neurons (31),

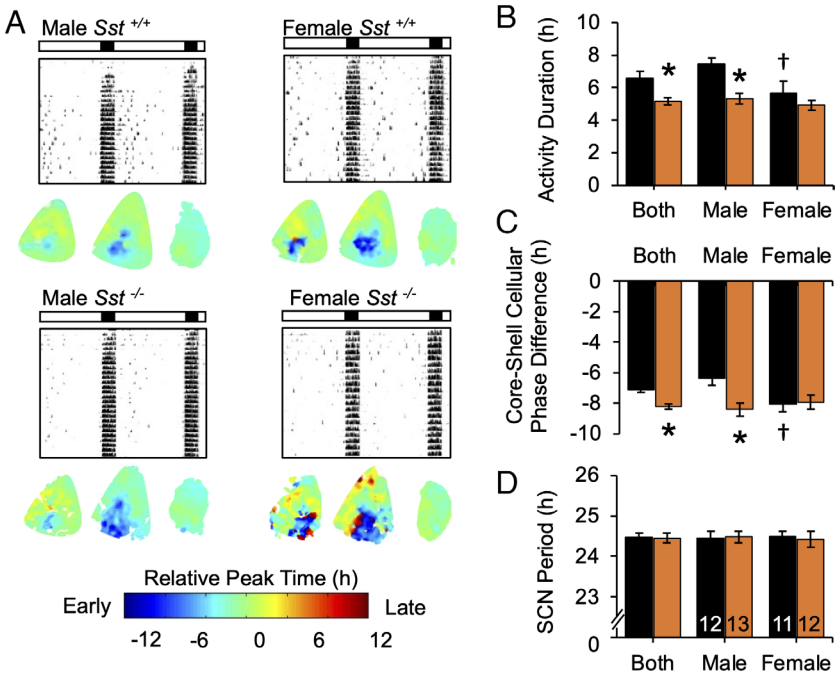

Fig. 6. Lack of SST enhances SCN encoding of long day photoperiods. (*A*) Representative double-plotted wheel-running actograms and individual SCN phase maps of mice entrained to L20 for 4 wk. (*B*) Lack of SST increased alpha compression in L20 males. (*C*) Lack of SST increased SCN reorganization in L20 males. (*D*) Lack of SST did not affect SCN period. †Wild-type sex difference, *Genotype difference, post hoc comparisons, $P < 0.05$.

but it has not been tested whether photoperiod induces epigenetic reprogramming in the SCN. In the PVN, light-driven neurotransmitter switching between SST and dopamine expression (17, 18) is induced by a subpopulation of SCN NMS neurons (20, 32) that coexpress VIP, AVP, or SST (9, 33). Given that VIP-, NMS-, and AVP-expressing SCN neurons regulate PVN function to modulate

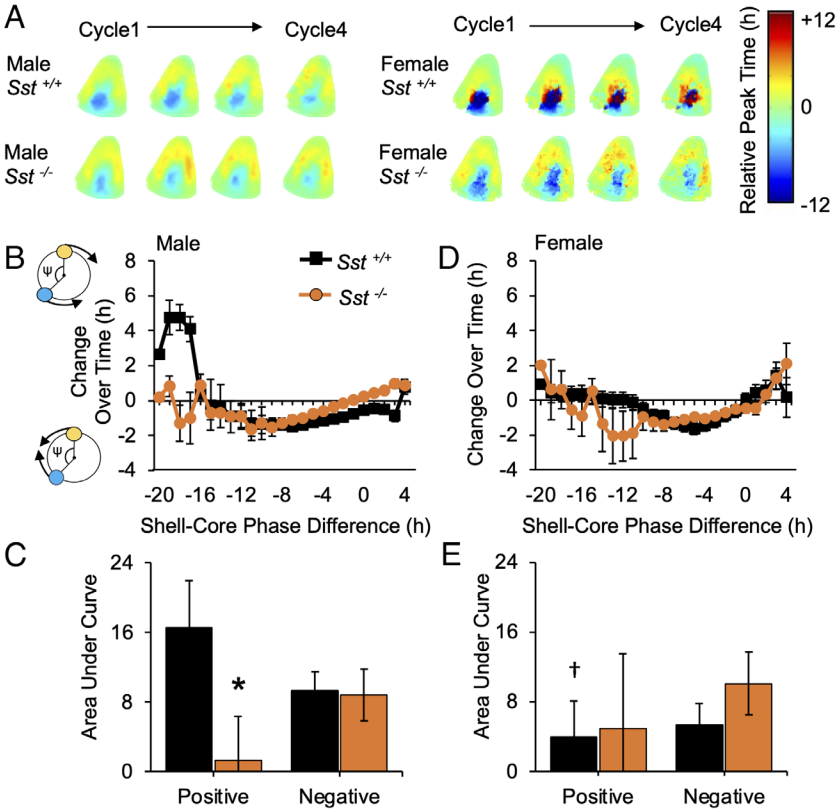

Fig. 7. Lack of SST and sex modulates SCN coupling after exposure to long days. (*A*) Composite phase maps for L20 SCN over time in culture. (*B*) Coupling response curves illustrating cellular resynchronization in male SCN. Polar plots along Y-axis illustrate that the sign of cellular responses reflects the direction of change over time in culture (blue: SCN core neurons, yellow: SCN shell neuron, ψ: phase difference angle). (*C*) Area under the curve for positive and negative regions of the coupling response curve for male SCN. (*D* and *E*) Coupling response curves and area under the curve for female SCN. Male n = 6 to 14 mice/genotype, Female n = 5 to 9 mice/genotype. *post hoc comparisons, $P < 0.05$.

daily rhythms in hormone synthesis, sleep, and affective behavior (34–37), future studies should test how SST signaling influences the physiology of different types of cells in the SCN network and the broader circadian system.

Deletion of *Sst* influenced circadian plasticity under three classic assays reflecting light-induced changes in SCN organization (13, 38–40). Under long and short days, $Sst^{-/-}$ mice displayed larger and/or faster changes in waveform of daily locomotor rhythms. In contrast, genotype did not affect daily rhythms under L12 or the photic PRC, indicating that retinal processing and SCN responses to discrete light pulses are intact in $Sst^{-/-}$ mice. Further, loss of *Sst* did not alter circadian period after DD release from any photoperiod, suggesting that SST signaling influences circadian mechanisms controlling the waveform of daily rhythms rather than period or phase (12, 13, 41). Collectively, this pattern of results suggests that SST is not necessary for intrinsic circadian timekeeping or stable photoentrainment, but instead that SST signaling increases circadian robustness after lighting conditions change. In line with this interpretation, loss of *Sst* also enhanced circadian responses to simulated jetlag and constant light, which likewise reflect SCN reprogramming (13, 38–40). Importantly, we find that genetic and pharmacological manipulation of SST signaling potentiated SCN responses to long days in a manner that aligns with the behavioral phenotype of $Sst^{-/-}$ mice. This is in agreement with previous work that establishes the necessity of the SCN in mediating circadian responses to light (42). Further, our pharmacological results and previous work (42) provide evidence that SST signaling can directly modulate SCN function. However, it remains possible that the behavioral phenotype of $Sst^{-/-}$ mice involves SST signaling in non-SCN structures, and future studies using conditional approaches will be useful in identifying the precise pathways by which SST signaling modulates how light affects daily rhythms in behavior and SCN function.

The present results highlight a potential network mechanism by which SST signaling in the SCN can regulate circadian responses to light, specifically by regulating neuropeptide expression in SCN core neurons. Notably, we find that *Sst* deletion increases the number of VIP and GRP neurons in the retinorecipient SCN core, which could serve to enhance circadian responses to light when the photic environment changes (8–10). In this manner, the effects of *Sst* deletion are unlike those of other SCN and retinal mutations that decrease neuropeptide expression and cause photic deficits (e.g., refs. 43 and 44). In the rat SCN, SST neurons have been shown to synapse onto VIP neurons, VIP dendrites, and GRP neurons (45, 46), which could modulate processing of retinal inputs by retinorecipient SCN neurons (47). In addition, depletion of SST in the rat SCN has been shown to unmask a daily VIP rhythm by increasing VIP expression during the daytime (48). Together with our current findings, this pattern of results suggests that SST signaling may influence circadian responses to light by inhibiting VIP/GRP expression in an expandable pool of SCN core neurons (*SI Appendix*, Fig. S10*E*). Overall, it is notable that both VIP and SST modulate similar circadian behaviors, from siestas to seasons (10, 11, 36). Photoperiod regulates SCN expression of both VIP and SST (present work, refs. 20 and 49), which may occur through parallel or multisynaptic pathways. A recent study found that long days increase SCN VIP expression within 2 wk (20), but we did not detect SCN de novo *Sst* transcription until after 6 to 8 wk of long day exposure. This suggests that photoperiod may initially modulate VIP expression, with later upregulation of SST coincident with the timing of SCN reorganization and photoentrainment stabilization (present results; ref. 13). Given that VIP is necessary for SCN timekeeping, photic resetting, and photoperiodic encoding (8–10), testing the molecular mechanisms by which SST signaling regulates VIP neurons represents an exciting direction for future research.

This work also expands insight into sex differences in SCN circuits that process light. Loss of SST affected the power of LL rhythms and photoperiodic alpha in both sexes, but significantly influenced siesta duration, jetlag recovery, and LL-induced arrhythmia only in males. Thus, there was SST dependence in both sexes, with a more limited phenotypic range in females. Notably, the SST knockout phenotype was specific to males under assays where there was a strong sex difference in wild-type mice. This provides evidence for sex convergence and divergence in the circadian system (50), where sex differences in neurobiological mechanisms produce similar behavioral end points under baseline conditions (convergence) and different responses to perturbation (divergence). Wild-type females recovered faster from simulated jetlag and displayed higher rates of LL-induced arrhythmia relative to males, consistent with previous work (28). Interestingly, *Sst* deletion eliminated this sex difference because $Sst^{-/-}$ males matched the behavioral and cellular responses seen in females. Likewise, we discovered that SCN network synchrony and intercellular coupling differ by sex, with loss of *Sst* eliminating this sex difference. The sex-influenced role of SST on SCN physiology may reflect sex differences in SST signaling and/or in downstream circuits. For instance, we found that SCN expression of SST/*Sst* was rhythmic only in males, although these results could be influenced by the temporal resolution of the time courses used here (i.e., 6 h) and/or estrous-induced variability in the timing of daily rhythms in females. In addition, the photoperiodic regulation of SST/*Sst* differed by sex in both the SCN and PeVN. Last, we detected sex differences in the number of SCN *Vip* neurons expressing *Sstr1*, as well as sexual variation in daily rhythms of *Sstr1, Vip,* and *Grp* expression. Given that VIP and GABA modulate SCN coupling in the cellular assay employed here (13), sex differences in SCN encoding and coupling could reflect variation in these downstream signaling pathways (*SI Appendix*, Fig. S10*E*). Overall, these data suggest that SST is integrated into clock circuits that differ by sex, consistent with previous work revealing sex differences in SCN neuropeptide expression and photic processing (28). Greater understanding of sex differences in clock circuits is an important future goal because men and women display differences in the effects of circadian disruption (51). Moreover, up to 80% of people who suffer from winter depression are women (52, 53), and women report being more seasonal (5, 54). Future work comparing photic processing in the brains of both sexes will be important to identify neurobiological factors influencing gender disparities in circadian clock function and light-driven disease.

Materials and Methods

Mice and Husbandry Conditions. Mice were bred and raised under a 24-h light–dark cycle with 12 h of light and 12 h of darkness [L12; lights off: 1800 CST defined as Zeitgeber Time 12 (ZT12)]. Both male and female mice were used in all experiments unless otherwise noted. All procedures were conducted according to the NIH Guide for the Care and Use of Animals and were approved by the Institutional Animal Care and Use Committees at Marquette University.

Genetic Labeling of SCN Neurons. To genetically label *Sst* neurons, Sst-IRES-Cre mice ((55), JAX#018973, C57Bl/6N background) were crossed to Ai9 mice (56). In progeny of this cross, Cre recombinase is expressed under the *Sst* promoter, causing cell-specific expression of the red fluorescent protein, tdTomato (tdT). This genetic approach permanently labels cells after *Sst* transcription regardless of continued expression or daily variation in peptide transcript expression. To compare the SCN *Sst*–tdT+ cells to those of other SCN peptide groups, Ai9 mice were also crossed to Vip-IRES-Cre mice ((55), JAX# 010908, C57Bl/Jx129S background) and Avp-IRES-Cre mice ((23), JAX# 023530, C57Bl/6 background).

IHC and In Situ Hybridization. *Sst*–tdT labeling in *Sst*-IRES-Cre$^{+/}$;Ai9$^{+/-}$ mice was complemented with SST IHC on tissue collected at ZT00, ZT06, ZT12, or ZT18. To test photoperiodic changes in overall SST expression, male and female PER2::LUC$^{+/+}$ mice were exposed to a photocycle with either 12 h, 18 h, or 6 h of light per day before receiving 1 μL colchicine injection into the third ventricle to slow microtubule transport and measure cumulative SCN SST expression over the circadian cycle using IHC. Anti-SST antibodies were validated in-house using male *Sst*$^{+/+}$ and *Sst*$^{-/-}$ mice (*SI Appendix*, Fig. S2*A*). To test that lack of SST alters SCN neurochemistry, *Sst*$^{+/+}$; *Sst*$^{+/-}$; and *Sst*$^{-/-}$;PER2::LUC$^{+/+}$ mice entrained to L12 were given 1 μL colchicine injections to analyze cumulative SCN expression of VIP, GRP, and AVP over the circadian cycle using IHC. RNA expression was assessed in wild-type mice using fluorescent in Situ hybridization and RNA Scope HiPlex assays conducted on tissue collected at ZT00, ZT06, ZT12, or ZT18. Processing of samples is described in detail in *SI Appendix, Methods*.

Circadian Behavioral Assays. Mice were transferred to individual cages equipped with a running wheel, with wheel-running data collected and analyzed using ClockLab software (Actimetrics, Wilmette, IL). To test whether SST modulates photoperiodic behavior, male and female *Sst*$^{+/}$;PER2::LUC mice, *Sst*$^{+/-}$;PER2::LUC mice, and *Sst*$^{-/-}$;PER2::LUC mice were entrained to L12, L20, or L04 for 10 wk, respectively, and then released into constant darkness (DD) to test free-running period and photic resetting to 20 min light pulses. To test whether SST affected response to simulated jetlag, male and female *Sst*$^{+/+}$ and *Sst*$^{-/-}$ mice were entrained to L12 prior to a 6 h advance of the light–dark cycle. To test whether SST modulates parametric responses to constant light, male and female *Sst*$^{+/+}$ and *Sst*$^{-/-}$ mice were transferred from L12 into constant light (LL). Analyses of circadian behavior are described in detail in *SI Appendix, Methods*.

PER2::LUC Assays. SCN slices (150 μm) were collected in the coronal plane using a vibratome and cultured as described previously (13). To test the effects of SSTR1 signaling on SCN timekeeping, the selective SSTR1 agonist CH275 (1 μM, Tocris Cat#2454) or volume-matched vehicle (DMEM) was applied directly to each SCN slice at ZT12 before luminometry recording for at least 4 d. To test how lack of SST influences SCN photoperiodic responses, male and female *Sst*$^{+/}$;PER2::LUC mice, *Sst*$^{+/-}$;PER2::LUC mice, and *Sst*$^{-/-}$;PER2::LUC mice were entrained to L12 or L20 for at least 4 wk. To test how SSTR antagonism influenced SCN photoperiodic responses, SCN slices were collected from male PER2::LUC mice and cultured with or without a broad-spectrum SSTR antagonist (20 μM, Tocris Cat#3493) for the duration of the experiment. Procedures used for recording and analyses are described in detail in *SI Appendix, Methods*.

Statistical Analysis. Data are represented in figures as mean ± SEM. Cosine curve-fitting was performed to detect significant daily rhythms using Circwave software (56). Other statistical analyses were performed with JMP software (SAS Institute, Cary, NC). When models contained within-subject factors (region, slice position, weeks), a mixed linear model was used to parse out random effects driven by individual differences among mice. When models only contained between-subject factors, a full-factorial ANOVA was used to assess the effects and interactions of one to four factors: 1) SST genotype, 2) photoperiod, 3) time of day, and/or 4) sex. Data were analyzed for each sex separately where appropriate. Post-hoc tests were performed with Tukey's HSD or least square mean contrasts to control for family-wise error. Statistical significance was set at $P < 0.05$.

Data, Materials, and Software Availability. All study data are included in the article and/or *SI Appendix*.

ACKNOWLEDGMENTS. We thank the Marquette University Animal Resource Center for animal care. For their assistance, we thank Brian Maunze, Niav O'Neill, Ina Ramos, Emily Herff, Mary Bozsik, Shabi Hader, Julie Zhu, Amanda Pastrick, Tori Montinola, Matthew Diaz, Adam Telega, Dr. Malcolm Low, and Stanford Photonics. Portions of this work were developed from the doctoral dissertation of D.A.M.J. This work was supported by the NIH, R01091234.

Author affiliations: [a]Department of Biomedical Sciences, Marquette University, Milwaukee, WI 53233

1. J. A. Evans, A. J. Davidson, Health consequences of circadian disruption in humans and animal models. *Prog. Mol. Biol. Transl. Sci.* **119**, 283–323 (2013).
2. T. M. McMenamin, A time to work: Recent trends in shift work and flexible schedules. *Mon. Labor. Rev.* **130**, 9–11 (2007).
3. F. Falchi *et al.*, The new world atlas of artificial night sky brightness. *Sci. Adv.* **2**, e1600377 (2016).
4. W. M. Sweileh, Analysis and mapping of global research publications on shift work (2012 to 2021). *J. Occup. Med. Toxicol.* **17**, 22 (2022).
5. A. Wirz-Justice, Seasonality in affective disorders. *Gen. Comp. Endocrinol.* **258**, 244–249 (2018).
6. M. H. Hastings, E. S. Maywood, M. Brancaccio, Generation of circadian rhythms in the suprachiasmatic nucleus. *Nat. Rev. Neurosci.* **19**, 453–469 (2018).
7. D. A. M. Joye, R. A. Wheeler, J. A. Evans, "Daily timekeeping, photic processing and photoperiodic encoding by the suprachiasmatic nucleus" in *Biological Implications of Circadian Disruption: A Modern Health Challenge*, L. K. Fonken, R. J. Nelson, Eds. (Cambridge University Press, in press).
8. J. R. Jones, T. Simon, L. Lones, E. D. Herzog, SCN VIP neurons are essential for normal light-mediated resetting of the circadian system. *J. Neurosci.* **38**, 7986–7995 (2018).
9. S. Wen *et al.*, Spatiotemporal single-cell analysis of gene expression in the mouse suprachiasmatic nucleus. *Nat. Neurosci.* **23**, 456–467 (2020).
10. A. M. Vosko, A. Schroeder, D. H. Loh, C. S. Colwell, Vasoactive intestinal peptide and the mammalian circadian system. *Gen. Comp. Endocrinol.* **152**, 165–175 (2007).
11. E. A. Lucassen *et al.*, Role of vasoactive intestinal peptide in seasonal encoding by the suprachiasmatic nucleus clock. *Eur. J. Neurosci.* **35**, 1466–1474 (2012).
12. J. Myung *et al.*, GABA-mediated repulsive coupling between circadian clock neurons in the SCN encodes seasonal time. *Proc. Natl. Acad. Sci. U.S.A.* **112**, E3920–E3929 (2015).
13. J. A. Evans, T. L. Leise, O. Castanon-Cervantes, A. J. Davidson, Dynamic interactions mediated by nonredundant signaling mechanisms couple circadian clock neurons. *Neuron* **80**, 973–983 (2013).
14. M. Tanaka *et al.*, Somatostatin neurons form a distinct peptidergic neuronal group in the rat suprachiasmatic nucleus: A double labeling in situ hybridization study. *Neurosci. Lett.* **215**, 119–122 (1996).
15. E. E. Abrahamson, R. Y. Moore, Suprachiasmatic nucleus in the mouse: Retinal innervation, intrinsic organization and efferent projections. *Brain Res.* **916**, 172–191 (2001).
16. L. C. Lin, E. Sibille, Somatostatin, neuronal vulnerability and behavioral emotionality. *Mol. Psychiatry* **20**, 377–387 (2015).
17. D. Dulcis, P. Jamshidi, S. Leutgeb, N. C. Spitzer, Neurotransmitter switching in the adult brain regulates behavior. *Science* **340**, 449–453 (2013).
18. J. W. Young *et al.*, Mice with reduced DAT levels recreate seasonal-induced switching between states in bipolar disorder. *Neuropsychopharmacology* **43**, 1721–1731 (2018).
19. S. P. Deats, W. Adidharma, L. Yan, Hypothalamic dopaminergic neurons in an animal model of seasonal affective disorder. *Neurosci. Lett.* **602**, 17–21 (2015).
20. A. Porcu *et al.*, Seasonal changes in day length induce multisynaptic neurotransmitter switching to regulate hypothalamic network activity and behavior. *Sci. Adv.* **8**, eabn9867 (2022).
21. C. Fukuhara, K. Shinohara, K. Tominaga, Y. Otori, S. T. Inouye, Endogenous circadian rhythmicity of somatostatin like-immunoreactivity in the rat suprachiasmatic nucleus. *Brain Res.* **606**, 28–35 (1993).
22. S. Panda *et al.*, Coordinated transcription of key pathways in the mouse by the circadian clock. *Cell* **109**, 307–320 (2002).
23. J. A. Harris *et al.*, Anatomical characterization of Cre driver mice for neural circuit mapping and manipulation. *Front. Neural Circuits* **8**, 76 (2014).
24. C. S. Pittendrigh, S. Daan, A functional analysis of circadian pacemakers in nocturnal rodents: V. Pacemaker structure: A clock for all seasons. *J. Comp. Physiol.* **106**, 333–355 (1976).
25. M. J. Low *et al.*, Somatostatin is required for masculinization of growth hormone-regulated hepatic gene expression but not of somatic growth. *J. Clin. Invest.* **107**, 1571–1580 (2001).
26. A. Albrecht *et al.*, Circadian modulation of anxiety: A role for somatostatin in the amygdala. *PLoS One* **8**, e84668 (2013).
27. J. C. Ehlen, S. Hesse, L. Pinckney, K. N. Paul, Sex chromosomes regulate nighttime sleep propensity during recovery from sleep loss in mice. *PLoS One* **8**, e62205 (2013).
28. D. A. M. Joye, J. A. Evans, Sex differences in daily timekeeping and circadian clock circuits. *Semin. Cell Dev. Biol.* **126**, 45–55 (2021).
29. S. Pinto *et al.*, Rapid rewiring of arcuate nucleus feeding circuits by leptin. *Science* **304**, 110–115 (2004).
30. D. Meng, H. Q. Li, K. Deisseroth, S. Leutgeb, N. C. Spitzer, Neuronal activity regulates neurotransmitter switching in the adult brain following light-induced stress. *Proc. Natl. Acad. Sci. U.S.A.* **115**, 5064–5071 (2018).
31. A. Azzi *et al.*, Network dynamics mediate circadian clock plasticity. *Neuron* **93**, 441–450 (2017).
32. R. A. Romanov *et al.*, Molecular interrogation of hypothalamic organization reveals distinct dopamine neuronal subtypes. *Nat. Neurosci.* **20**, 176–188 (2017).
33. I. T. Lee *et al.*, Neuromedin S-producing neurons act as essential pacemakers in the suprachiasmatic nucleus to couple clock neurons and dictate circadian rhythms. *Neuron* **85**, 1086–1102 (2015).
34. D. Ono *et al.*, The mammalian circadian pacemaker regulates wakefulness via CRF neurons in the paraventricular nucleus of the hypothalamus. *Sci. Adv.* **6**, eabd0384 (2020).
35. A. Kalsbeek, E. Fliers, M. A. Hofman, D. F. Swaab, R. M. Buijs, Vasopressin and the output of the hypothalamic biological clock. *J. Neuroendocrinol.* **22**, 362–372 (2010).
36. B. Collins *et al.*, Circadian VIPergic neurons of the suprachiasmatic nuclei sculpt the sleep-wake cycle. *Neuron* **108**, 486–499.e485 (2020).
37. S. Paul *et al.*, Output from VIP cells of the mammalian central clock regulates daily physiological rhythms. *Nat. Commun.* **11**, 1453 (2020).
38. H. Ohta, S. Yamazaki, D. G. McMahon, Constant light desynchronizes mammalian clock neurons. *Nat. Neurosci.* **8**, 267–269 (2005).
39. N. Inagaki, S. Honma, D. Ono, Y. Tanahashi, K. Honma, Separate oscillating cell groups in mouse suprachiasmatic nucleus couple photoperiodically to the onset and end of daily activity. *Proc. Natl. Acad. Sci. U.S.A.* **104**, 7664–7669 (2007).
40. M. T. Sellix *et al.*, Aging differentially affects the re-entrainment response of central and peripheral circadian oscillators. *J. Neurosci.* **32**, 16193–16202 (2012).

41. M. C. Tackenberg, J. J. Hughey, D. G. McMahon, Distinct components of photoperiodic light are differentially encoded by the mammalian circadian clock. *J. Biol. Rhythms.* **35**, 353–367 (2020).
42. T. Hamada, S. Shibata, A. Tsuneyoshi, K. Tominaga, S. Watanabe, Effect of somatostatin on circadian rhythms of firing and 2-deoxyglucose uptake in rat suprachiasmatic slices. *Am. J. Physiol.* **265**, R1199–R1204 (1993).
43. J. L. Bedont *et al.*, Asymmetric vasopressin signaling spatially organizes the master circadian clock. *J. Comp. Neurol.* **526**, 2048–2067 (2018).
44. L. Ruggiero, C. N. Allen, R. L. Brown, D. W. Robinson, Mice with early retinal degeneration show differences in neuropeptide expression in the suprachiasmatic nucleus. *Behav. Brain Funct.* **6**, 36 (2010).
45. M. Maegawa *et al.*, Differential immunolabeling for electron microscopy of diverse peptidergic neurons. *J. Histochem. Cytochem.* **35**, 251–255 (1987).
46. H. J. Romijn, A. A. Sluiter, C. W. Pool, J. Wortel, R. M. Buijs, Evidence from confocal fluorescence microscopy for a dense, reciprocal innervation between AVP-, somatostatin-, VIP/PHI-, GRP-, and VIP/PHI/GRP-immunoreactive neurons in the rat suprachiasmatic nucleus. *Eur. J. Neurosci.* **9**, 2613–2623 (1997).
47. J. Urban-Ciecko, A. L. Barth, Somatostatin-expressing neurons in cortical networks. *Nat. Rev. Neurosci.* **17**, 401–409 (2016).
48. C. Fukuhara, T. Nishiwaki, F. R. Cagampang, S. T. Inouye, Emergence of VIP rhythmicity following somatostatin depletion in the rat suprachiasmatic nucleus. *Brain Res.* **645**, 343–346 (1994).
49. M. J. Duncan, X. Cheng, K. S. Heller, Photoperiodic exposure and time of day modulate the expression of arginine vasopressin mRNA and vasoactive intestinal peptide mRNA in the suprachiasmatic nuclei of Siberian hamsters. *Brain Res. Mol. Brain Res.* **32**, 181–186 (1995).
50. M. M. McCarthy, A. P. Arnold, G. F. Ball, J. D. Blaustein, G. J. De Vries, Sex differences in the brain: The not so inconvenient truth. *J. Neurosci.* **32**, 2241–2247 (2012).
51. N. Santhi *et al.*, Sex differences in the circadian regulation of sleep and waking cognition in humans. *Proc. Natl. Acad. Sci. U.S.A.* **113**, E2730–E2739 (2016).
52. A. Magnusson, An overview of epidemiological studies on seasonal affective disorder. *Acta psychiatr. Scand.* **101**, 176–184 (2000).
53. S. Melrose, Seasonal affective disorder: An overview of assessment and treatment approaches. *Depress. Res. Treat.* **2015**, 178564 (2015).
54. L. M. Lyall *et al.*, Seasonality of depressive symptoms in women but not in men: A cross-sectional study in the UK biobank cohort. *J. Affect. Disord.* **229**, 296–305 (2018).
55. H. Taniguchi, Genetic dissection of GABAergic neural circuits in mouse neocortex. *Front. Cell. Neurosci.* **8**, 8 (2014).
56. L. Madisen *et al.*, A robust and high-throughput Cre reporting and characterization system for the whole mouse brain. *Nat. Neurosci.* **13**, 133–140 (2010).